

Polymer concrete filled circular steel beams subjected to pure bending

Walter O. Oyawa†

Department of Civil Engineering, JKUAT, P.O. Box 62000-00200, Nairobi, Kenya

Kunitomo Sugiura‡ and Eiichi Watanabe‡†

Department of Civil and Earth Resources Engineering, Kyoto University, Kyoto, 606-8501, Japan

(Received October 23, 2003, Accepted July 27, 2004)

Abstract. In view of the mounting cost of rehabilitating deteriorating infrastructure, further compounded by intensified environmental concerns, it is now obvious that the evolvement and application of advanced composite structural materials to complement conventional construction materials is a necessity for sustainable construction. This study seeks alternative fill materials (polymer-based) to the much-limited cement concrete used in concrete-filled steel tubular structures. Polymers have been successfully used in other industries and are known to be much lighter, possess high tensile strength, durable and resistant to aggressive environments. Findings of this study relating to elasto-plastic characteristics of polymer concrete filled steel composite beams subjected to uniform bending highlight the enormous increase in stiffness, strength and ductility of the composite beams, over the empty steel tube. Moreover, polymer based materials were noted to present a wide array of properties that could be tailored to meet specific design requirements e.g., ductility based design or strength based design. Analytical formulations for design are also considered.

Key words: composite section; polymer concrete; flexural strength.

1. Introduction

Contemporary structural engineering practice has for a long time employed the traditional materials, steel and reinforced concrete as the key construction materials, despite their structural limitations or even their inadequacy in assuaging rising environmental concerns in recent times. Concern and worries abound over the enormous cost of rehabilitating dilapidated or old reinforced concrete structures; some countries like the USA and Japan are already spending colossal amounts of money in the rehabilitation or replacement of old reinforced concrete structures. It is no wonder that in this new century, sustainable construction is becoming an overriding consideration, where advanced composite formulations and systems of re-defined performance are being vigorously sought (Bentur 2002). Indeed the construction industry is already in a new era where not only is there interest in the expansion of mankind's frontiers into the realm of new technologies, but also the need for a harmonious co-existence with the eco-sphere

†Senior Lecturer

‡Associate Professor

‡†Professor

by minimizing damage to the natural environment and optimizing material technology and infrastructure to create a healthy life in harmony with nature. In particular, the cement industry has taken the lead in developing “eco-cement”, a product that helps clean the environment by utilizing municipal solid wastes in its manufacture and is even said to have the potential of absorbing CO₂ from the environment as it hydrates. The concept of eco-materials (ecologically-benign materials) has been introduced to encourage the development of materials that are not only harmless to the global environment but also exert minimal burden on the planet during their production, by making efficient use of raw materials and being highly recyclable.

In addition to seeking strong and/or ductile materials for seismic resistance (Kawashima and Unjoh 1997, Shams and Ala 1997), this study was motivated by the cutting edge concept of durable and eco-friendly materials for sustainable development and was directed towards evaluating the suitability of polymer-based materials such as polymer concrete, for use as fill materials in filled steel composite members. Polymers or polymer based materials have been successfully used in other industries and are attracting increased attention in the construction industry due to the complementary properties to concrete that they possess viz higher tensile capacity and ductility, lower weight, high damping or resilience, and resistance to physical and chemical attack that ensures their longevity or durability (Fowler 1999, Kardon 1997, Ohama 1987). They were first introduced to hydraulic-cement systems in 1923 because of an increased need at that time for durable construction materials (Sujavanich and Lundy 1998). Although the cost of polymers may be comparatively high at present, a situation attributed to their use in other highly lucrative industries such as the defense and aerospace industries, it is envisaged that continued research directed towards seeking optimal conditions and cheap derivatives e.g., municipal wastes (Rebeiz and Mielich 1995, Rebeiz and Fowler 1996, Solovjov *et al.* 1994) for use specifically in the construction industry will eventually lead to satisfactory cost reduction. Moreover, the trend towards the evaluation of full life-cycle cost of structures (Hastak and Halpin 2000), to include such parameters as maintenance, repair, demolition and environmental degradation, rewardingly place the durability of polymer based materials at the forefront of cost analysis.

Previous tests have already been conducted concentrating on the behaviour of different types of filled steel composite stub columns subjected to compressive load and also composite beams filled with fibre latex cement mortar and pure epoxies (Oyawa *et al.* 1998, 1999, 2001). Results obtained indicate the great potential of fibre latex-cement mortar and epoxies as alternative fill materials to cement concrete or which could be combined with cement concrete to form advanced composites for enhanced strength, ductility and durability. This present work is a sequel to the above mentioned study, and focuses on the flexural behaviour, namely moment-curvature relations as well as cross-sectional strain and stress distributions, of different types of filled steel composite beams.

2. Experimentation

2.1. Outline of experimental program

Circular filled steel composite beams filled with various types of fill materials were gradually subjected to two-point bending load until limiting load or deformation was attained, while recording load, strain and displacement measurements for curvature determination, at suitable increments. The variable parameters were the outer radius to thickness ratio of the steel tube expressed as $D/2t$, where D is the outer diameter of the steel tube and t is the thickness, and three different types of fill materials. The ratio of effective

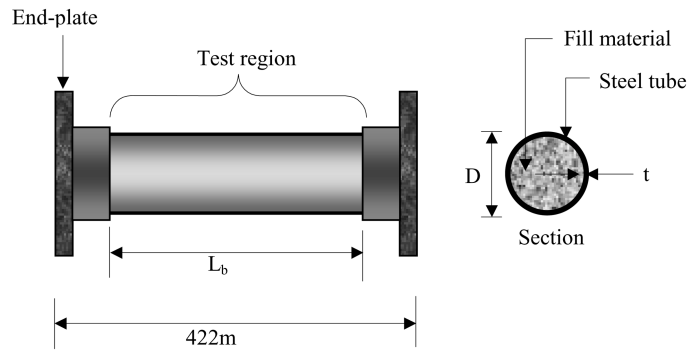


Fig. 1 Specimen, with fixing end-plates

Table 1 Beam specimen details (nominal)

Specimen label	Fill material	L_b (mm)	D (mm)	t (mm)	L_b/D	$D/2t$
S/E1A-30B	Epoxy concrete-HS	288	96	1.6	3	30
S/E2A-30B	Epoxy concrete-LS	288	96	1.6	3	30
S/CN-30B	Normal concrete	288	96	1.6	3	30
S-30B	-	288	96	1.6	3	30
S/E1A-50B	Epoxy concrete-HS	300	100	1.0	3	50
S/E2A-50B	Epoxy concrete-LS	300	100	1.0	3	50
S/CN-50B	Normal concrete	300	100	1.0	3	50
S-50B	-	300	100	1.0	3	50

Nomenclature: Specimen identification e.g. S/E1A-50B implies composite beam specimen of steel (S) filled with epoxy polymer concrete of high stiffness, of $D/2t$ ratio equal to 50 and tested in bending (B).

Abbreviations: HS-High stiffness LS-Low stiffness

length-to-diameter of steel tube (that is the L_b/D ratio) was maintained constant at 3. The three fill materials investigated were epoxy polymer concrete of high stiffness (E1A), epoxy polymer concrete of low stiffness (E2A) and normal concrete (CN). The epoxy concretes were special products from a manufacturer. In addition, empty circular steel beams were also tested.

Fig. 1 shows a typical specimen, while a summary of the testing program and details is presented in Table 1. To facilitate identification, the test specimens for bending test were designated according to material type and the value of radius to thickness ratio of the steel tube as is illustrated in the nomenclature below Table 1. Preparation of each of the filled steel composite specimens involved mixing of the constituents of the relevant fill material, followed by filling the steel tube with the mixture. The specimens were then left to cure up to the required day of testing. Specimens were tested after about one month (epoxies normally gain 90% of their full strength within 7 days).

2.2. Material properties

Fundamental properties of the fill materials used in this study were determined from compressive tests conducted on 100-mm-diameter by 200-mm-length cylindrical specimens. During the tests, compressive axial load provided by a 1000 KN capacity universal testing machine, was applied gradually on the top surface of each specimen which had been suitably capped to produce a nearly flat surface by means of

Table 2 Properties of the fill materials

Fill material description	Fill material designation	Unit weight (Kg/m ³)	Young's modulus (KN/mm ²)	Poisson's ratio	Ultimate strength (N/mm ²)	Strain at ultimate strength (%)	Bulk modulus (KN/mm ²)
Epoxy concrete-HS	E1A	2054	12.9	0.316	52.0	0.7208	11.7
Epoxy concrete-LS	E2A	2114	3.0	0.480	19.0	4.845	25.0
Normal concrete	CN	2326	29.6	0.171	26.0	0.4035	15.0

Abbreviations: HS-High stiffness LS-Low stiffness

Table 3 Properties of steel

Thickness (mm)	Young's modulus (KN/mm ²)	Poisson's ratio	Yield stress (N/mm ²)	Yield strain (%)	Ultimate strength (N/mm ²)	Elongation at break (%)	Bulk modulus (KN/mm ²)
1.6	216	0.347	225	0.1042	325	46.9	235
1.0	211	0.337	230	0.1092	340	42.8	216

fitting steel plates. Data monitored, included longitudinal and horizontal strains through appropriate strain gages for each material, bonded to the middle circumference of each specimen, axial shortening as measured by four linear variable displacement transducers (LVDTs) between the loading heads and fixed equidistant around the specimen, and the applied load as monitored from the load meter. The data were monitored by a computer via a connection to a data logger. Accordingly, ultimate strength was obtained as the ultimate load per cross-sectional area, Young's modulus (E) as the initial tangent gradient of the load-axial strain curve, and Poisson's ratio (ν) as the ratio of the lateral strain to the longitudinal strain. Bulk modulus (K), regarded as a measure of incompressibility of the fill material, was determined from the expression $K=E/3(1-2\nu)$. Table 2 gives the properties and characteristics of the fill materials.

As for the enclosing steel shell, SS400 grade steel was used. Material properties for the two different thickness sizes of steel used were determined from tensile tests on strips cut from steel sheets used to form the tubes. Test strips with a test region of about 15 mm width and 75 mm height and grip length of 25 mm width and 70 mm height at both ends, were each tested by clamping between the heads of the Universal Testing Machine and applying constant load rate while monitoring the axial and lateral strains as well as the applied load through a data logger connected to a computer. Results obtained are shown in Table 3.

2.3. Test set-up and loading

Bending tests were carried out on six filled steel composite beams and two empty steel beams. The beam tests were in two series formed from tubular steel pipes of radius/thickness ratio ($D/2t$) of 30 and 50, and for each of the series several fill materials were involved. A specimen for test was first instrumented with seven equally spaced strain gages circumferentially on one side at the mid-span. The circular specimen having rectangular rigid end plates was then firmly bolted to rigid rectangular steel attachments at either end. The whole mass was in turn rested on simple supports fixed to a firm rigid beam base as shown in Fig. 2. The setup was supported and aligned on the bottom platen of 1000 KN capacity universal testing machine. Two linear variable displacement transducers (LVDTs) with

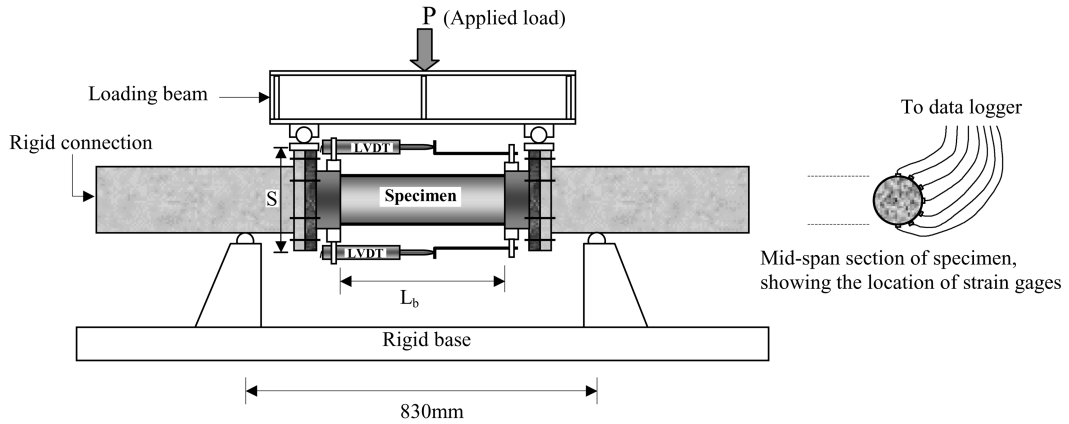


Fig. 2 Test set-up before loading

magnetic bases were fixed, one at the top and one at the bottom of the beam, in such a way as to measure the relative horizontal movement between two known points of gage length (L_b) in order to determine the average curvature. The vertical distance (S) between the LVDTs was recorded for every test.

A two-point load supplied by the universal testing machine through a rigid loading beam as shown in Fig. 2 on the specimen was meant to induce a state of pure bending in the test region. The loading beam and its attachments had to be securely clamped to prevent possible disastrous consequences. A slow loading application was used to avoid abrupt jolting loads. Loading then proceeded gradually and at suitable constant increment the applied load, as well as displacements of the LVDT heads and strains, as monitored by a computer via a data logger, were recorded. The constant incremental load rate was followed until the anticipated yield point of steel, following which the measurement time interval was reduced. Loading was continued beyond the peak load up to a stage where it was judged that no further useful information could be obtained from the test results. Failure load was taken as the peak load after the specimen shed off any additional load increment.

3. Results and discussions

3.1. Moment - curvature relationships

The moment-curvature relationship of a short beam or column is of prime importance in the analysis of any long beam-column, providing required parameters such as the stiffness of the beam-column. For the case of composite beams, other uncertain phenomena such as sectional interaction, interface slip and cracking of the fill material come into play, and may be manifested in the moment-curvature response. The obtained normalized moment-curvature relationships (from idealized representation in Fig. 3) are presented in Fig. 4, the summary of which is given in Table 4. The moment (M) for any applied load (P) can be obtained from the expression:

$$M = PL_a / 2 \quad (1)$$

and curvature (ϕ), rotation per unit length, is derived from the expression;

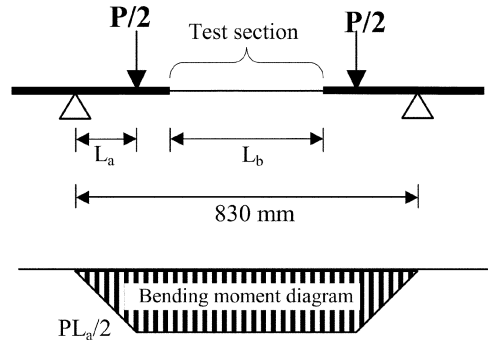


Fig. 3 Schematic representation of structural and loading conditions

$$\phi = (-U_{top} + U_{bottom}) / (S \cdot L_b) \quad (2)$$

where L_a is the distance from the beam support to the point of load application on the beam assuming symmetry of loading; U_{top} and U_{bottom} are displacements measured by the top and bottom LDVTs respectively; L_b is test section length; and S is the vertical distance between the two LDVTs.

Schematic representation of the structural and loading conditions shown in Fig. 3 implies that the test section should be subjected to a state of pure bending. Accordingly, the assumptions and theories of pure bending may be expected to apply to the elastic structural behaviour of the beam specimens, e.g., plane sections before bending should remain plane even after bending.

The yield moment (M_y) and yield curvature (ϕ_y) can be determined from the expression:

$$M_y = \frac{\sigma_{sy} I_s}{y_e} \quad (3)$$

$$\phi_y = \frac{\sigma_{sy}}{E_s y_e} \quad (4)$$

where, σ_{sy} = yield strength of steel

I_s = moment of inertia of the empty steel tube

y_e = distance from the elastic neutral axis of the circular cross-section of empty steel tube to the extreme point

E_s = modulus of elasticity of steel

Several distinct features may be observed from the results presented in the figures. First and foremost, the superior strength and ductility of composite beams vis-à-vis the empty steel tube is evident. This clearly depicts the beneficial interaction between the steel tube and the fill material. The confined fill material considerably delays local buckling of the steel tube on the compression side, only permitting minor outward local deformations in the post-yield response, thereby inducing the extensive exploitation of the bottom tensile yield strength of the steel tube. In other words, although these composite specimens were observed to have undergone considerable plastic deformations in bending, they continued to resist load because local buckling in the steel tube was strictly limited by the presence of the fill material, consequently resulting in increased strength and ductility. Increase in strength and ductility due to the presence of fill material has been observed for concrete-filled steel beams by other researchers. Particularly, it was recognized that the restriction of longitudinal movement of the fill material by providing end

plates or intermediate diaphragms significantly affects ductility (Ohtani and Matsui 1997). The general shape of the composite beam curves depicts an initial elastic linear portion, followed by a change in slope as the steel yields and transfers some of its load to the fill material in the compression zone. When this transfer stabilizes, the hardening gradient takes a near linear gradient again as the confined fill material in the compression zone takes up most of the load, while the stretched steel in the tension zone resists most of the tensile load.

The highest overall performance in terms of stiffness, strength and ductility is that shown by epoxy concrete filled beam (S/E1A), illustrating the great potential of polymer concrete as an alternative or supplementary material to ordinary cement concrete. The performance of S/E1A is even better than that of composite beam of pure epoxy S/E1 observed in previous work (Oyawa *et al.* 1999), and it has the added advantage in that epoxy concrete it is comparatively cheaper than pure epoxy formulation due to reduced resin content. A similar observation is made in the case of S/E2A and its corresponding epoxy filled steel beam S/E2 (Oyawa *et al.* 1999) where epoxy concrete-filled beam (S/E2A) has higher strength and ductility than epoxy-filled (S/E2). However, the polymer concretes are much heavier than the pure polymers, having weights that are close to that of ordinary cement concrete. Accordingly, in constructions where low weight of the fill material is desirable such as the construction of composite railway beams or retrofitting of hollow steel structures, pure polymers are preferable over polymer concrete. On the other hand, where weight is of less concern, then polymer concretes are definitely preferable over pure polymers due to their cheaper cost. It is evident that depending on the needs of construction, polymers or polymer composites may be suitably adjusted to meet the specific requirements, highlighting the versatility of polymers and polymer based materials. Previous studies on epoxy filled steel stub columns (Oyawa *et al.* 1998, 2001) gave interesting results in that a particular type of epoxy and epoxy concrete produced composite columns that showed considerable increase in ductility but only nominal increase in strength. This is very desirable in the current seismic design methods, because foundation structures of lesser size and cheaper cost can be used (Kitada 1998, Nakanishi *et al.* 1999). The advantage is most magnified in the retrofitting of structures where modifications in foundations are most unwelcome from economic point of view. In other words, the ductility of bridge piers needs to be increased without increasing their yield strength for the sake of economic design (Nakanishi *et al.* 1999).

Elsewhere in the world, many design codes now recommend two levels of design seismic force in that structures should be able to resist moderate earthquakes without structural damage, and be able to resist severe earthquakes without collapse but perhaps with some structural and non-structural damage. To satisfy these performance criteria, all structures should be designed to have adequate strength and stiffness to meet the serviceability limit states when responding to moderate earthquakes, and to have adequate strength, stiffness and ductility to satisfy the ultimate limit states when responding to severe earthquakes. Under severe seismic attack, the emphasis is on high ductility structures, designed employing equal energy (constancy) assumption. Polymer-based materials are best suited to take on this challenge, even when used as a replacement for cement concrete in ordinary reinforced concrete works. Studies by Abdel-Fattah and El-Hawary (1999) on the flexural behaviour of polymer concrete also concluded that polymer concrete beams are very ductile.

Table 4 provides a quantified summary of the flexural response of the tested beams, with the unique values shown in bold numbers. The table confirms the observations noted in Fig. 4 such as the higher elastic stiffness of S/CN specimen, while the epoxy specimens S/E1A and S/E2A give higher hardening stiffness and ductility. Table 4 further shows a dramatic reduction in hoop/axial strain ratio of concrete-filled steel beams (S/CN) in the bottom tensile zone. This is thought to be due to the low tensile strength of the stiff concrete, thus initiating early cracking with consequent haphazard expansion of the concrete

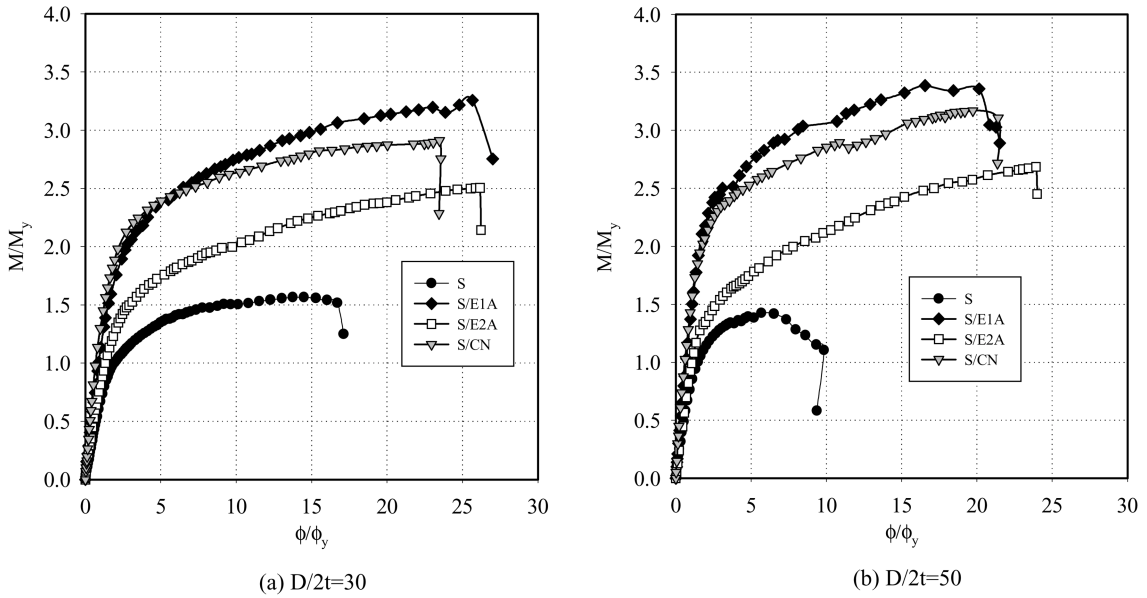
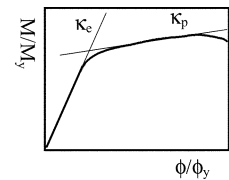


Fig. 4 Normalized moment-curvature relationships

Table 4 Summary of bending test results

Specimen label	Elastic stiffness κ_e	Hardening stiffness κ_p	M_{ult} / M_y	ϕ_{ult} / ϕ_y	Hoop/axial strain ratio on beam surface			
					Top of the beam		Bottom of the beam	
					ν_e	ν_p	ν_e	ν_p
S-30B	0.645	0.0228	1.57	14.0	0.335	0.563	0.389	0.828
S/E1A-30B	1.207	0.0308	3.26	25.7	0.349	0.709	0.387	0.202
S/E2A-30B	1.00	0.0334	2.51	26.2	0.378	0.679	1.319	0.563
S/CN-30B	1.65	0.0282	2.91	23.5	0.348	0.789	0.098	0.071
S-50B	0.807	early buckle	1.43	5.88	0.345	0.690	0.342	0.638
S/E1A-50B	1.57	0.0500	3.40	17.0	0.346	0.730	0.365	0.0402
S/E2A-50B	0.966	0.0464	2.69	23.9	0.468	0.753	0.458	0.482
S/CN-50B	2.04	0.0394	3.17	19.7	0.390	0.853	0.130	0.020

Note: κ_e and κ_p are as defined in the side Fig., while ν_e and ν_p represent the elastic and plastic values of the hoop/axial strain ratio, respectively.



and redistribution of stress possibly leading to biaxial tension in the bottom tensile zone of the steel tube. The effect of low tensile strength of concrete is vividly demonstrated, as it results in non-uniform interaction with the steel tube. It is also noted that the composite effect of filled beams is most realized for the thinner steel tube of $D/2t=50$, where both the elastic and hardening stiffness are higher than that for $D/2t=30$. Steel tube of $D/2t=50$ being the thinner steel tube is more susceptible to rapid buckling in the absence of fill material, hence the delay of local buckling by the fill material is more effective.

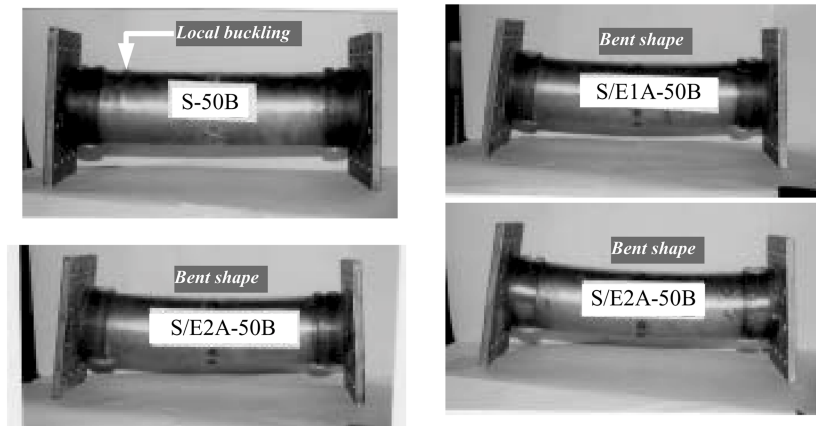


Fig. 5. Buckling and plastic bending deformations of the beam specimens ($D/2t = 50$)

3.2. Buckling deformations

Fig. 5 displays the buckling and plastic bending deformations of some of the tested specimens. Local buckling on the compression side is clearly visible in the case of the empty steel beam (S-50), where the buckling occurs in the form of ripples at the ends. However, for the composite beams, permanent bent or curved shape of the whole specimen results illustrating the moderating effect of fill material as it interacts with the steel tube. This interaction between the fill material and the enclosing steel tube limits buckling deformations in the steel tube, and in addition prevents ovalization of the tube as load is applied on the top. In general, two modes of deformation are known to manifest themselves in the buckling of empty uniform cylindrical shells acted upon by moments at their extreme ends. The first is the Brazier effect, which involves increasing ovalization of the cylindrical cross-section with increasing moment, with the result that the moment-curvature relationship is nonlinear; and the moment eventually reaches a maximum or limit value. The second type of deformation is termed the bifurcation buckling whereby axial waves form along the length of the cylinder, having maximum amplitude at the extreme compression side of the shell and gradually around the circumference (Reddy 1979). In a real situation, it must be expected that both these effects will be present simultaneously with one or the other dominating, depending on the proportions of the tube and the distribution of initial imperfections.

3.3. Analytical formulations and design implications

Design provisions for composite structures have generally been derived from conventional reinforced concrete or steel structures, mainly due to inadequate understanding of inelastic behaviour of composite members and systems. Whichever the method, applications are usually found in computing the response of a section to different load histories whereby the section model returns the moment-curvature response, or to carrying out the state of a section (integration point) in a frame element, whereby the section model returns the section forces that correspond to given section deformations e.g., axial strain and curvature. Two basic approaches are generally used to find the response of a composite section, viz, resultant models and fiber section models (Spacone and El-Tawil 2004). Resultant models explicitly define section responses in terms of moment-curvature response, axial load-axial strain relation, etc. In fiber section model the section is subdivided into small elements and the stresses are integrated over the

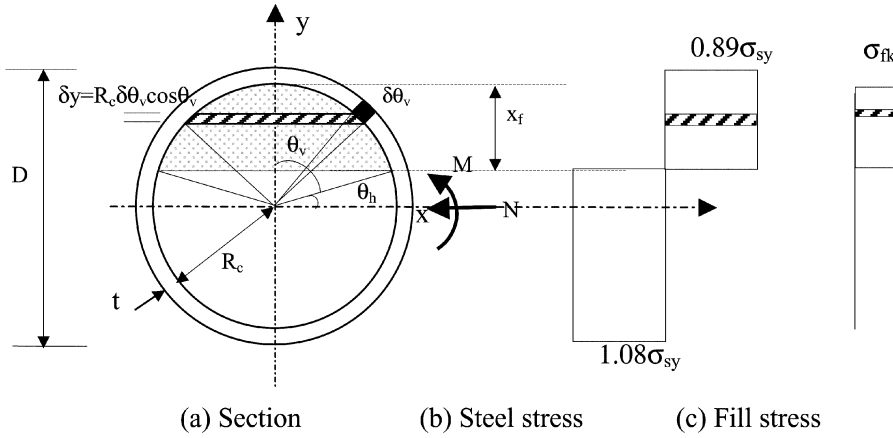


Fig. 6 Stress distribution recommended by AIJ

cross-sectional area to obtain stress resultants such as force or moment.

There is not universally accepted approach for the determination of bending strength (M_u) of circular filled steel composite beams, hence several design codes exist. The Architectural Institute of Japan (AIJ) in its release (1997) considers the confinement effect where the fill material strength in compression is enhanced while the strength of the encasing steel tube is appropriately factored in tension and compression zones to cater for the effect of hoop stresses induced by the fill material. The strengths are then determined assuming full plastic state in both the fill material and the steel tube as shown in Fig. 6.

Thus for equilibrium

$$N_u = \int_{A_f} \sigma_f dA_f + \int_{A_s} \sigma_s dA_s$$

$$M_u = \int_{A_f} \sigma_f Z_f dA_f + \int_{A_s} \sigma_s Z_s dA_s \quad (5)$$

which on substitution for the case of circular cross-section gives;

$$N_u = {}_f N_u + {}_s N_u = R_c^2 (\theta_v - \sin \theta_v \cos \theta_v) \sigma_{fc} + 2 \left(\frac{D}{2} - \frac{t}{2} \right) t (\beta_1 \theta_v + \beta_2 \theta_v - \pi) \sigma_{sy} \quad (6)$$

From which θ_v can be determined by ensuring equilibrium, followed by M_u as below;

$$M_u = {}_f M_u + {}_s M_u = \frac{2}{3} R_c^3 \sin^3 \theta_v \sigma_{fc} + 2 \left(\frac{D}{2} - \frac{t}{2} \right)^2 t (\beta_1 + \beta_2) \sin \theta_v \sigma_{sy} \quad (7)$$

where $\sigma_{fc} = 0.85 \sigma_{fk} + 0.78 \left(\frac{2t}{D-2t} \right) \sigma_{sy}$

M_u = Ultimate bending strength; N_u = Ultimate axial load; σ_{fc} = Confined strength of fill material; σ_{fk} = Unconfined strength of fill material; σ_{sy} = Yield strength of steel

In 1999, the Joint committee of steel-concrete composite structures of the JSCE (1999) released guidelines similar to AIJ entitled “Theory and design of steel concrete hybrid structure” and is mainly targeted to assist in the design of filled steel members for bridge construction. Like AIJ, full sectional plasticity is assumed and elemental forces are summed, while ensuring equilibrium. The very minor difference in the analytical procedure is that the distance from the circular section center to the steel elemental area is taken as $Rc + t/2$ in the case of AIJ while JCC takes it as Rc . Eqs. (8) and (9) give the expressions for the ultimate axial (N_u) and bending (M_u) strengths for circular section as determined by the JCC method.

$$\begin{aligned}
 N_u &= 2R^2 \sigma_f \int_{\alpha}^{\pi/2} \cos^2 \theta_h d\theta_h + 2Rt \sigma_{sy} \left(\int_{\alpha}^{\pi/2} d\theta_h - \int_{-\pi/2}^{\alpha} d\theta_h \right) \\
 &= \frac{\pi R^2 \sigma_{fc}}{2} \left(1 - \frac{2\alpha}{\pi} - \frac{\sin 2\alpha}{\pi} \right) - 4Rt \sigma_{sy} \alpha
 \end{aligned} \quad (8)$$

From which α can be determined by ensuring equilibrium, followed by M_u as below;

$$\begin{aligned}
 M_u &= 2R^3 \sigma_f \int_{\alpha}^{\pi/2} \sin \theta_h \cos^2 \theta_h d\theta_h + 2R^2 t \sigma_{sy} \left(\int_{\alpha}^{\pi/2} \sin \theta_h d\theta_h - \int_{-\pi/2}^{\alpha} \sin \theta_h d\theta_h \right) \\
 &= \frac{2R^3 \sigma_{fc}}{3} \cos^3 \alpha + 4R^2 t \sigma_{sy} \cos \alpha
 \end{aligned} \quad (9)$$

The applicability of the above equations is tested on the experimental results obtained in this study as given in Fig. 9. It is clearly evident that the AIJ and JCC methods used in the prediction of the ultimate bending moment of filled steel beams overly underestimates their strength i.e., they are very conservative and insensitive to the actual response of the composite beam. For example the stress configuration used implies simultaneous occurrence of ultimate stresses in the steel and fill material thus neglecting the benefits gained by plasticity of steel. Further, even though some of the fill materials e.g., concrete have negligible tensile strength there may be some effect generated by frictional interface interaction between the cracked fill material and the steel tube. Moreover, for beams confined with end-plates as is the case in this study, the beneficial effects of confinement are not well accounted for.

In view of the seeming underestimation of strength by the conventional methods, fiber section method is proposed which allows for non-concurrent attainment of ultimate conditions in the steel and fill material, and accounts for tension stiffening in the fill material. The fiber section method is a powerful tool that can be used to estimate the cross-sectional strength for design purposes. The method employs an iterative process in the calculation of forces and moments in the materials forming the section. The section is suitably divided into small elemental strips of known thickness (δy) in the case of the fill material and small elements of known subtended angle at the center ($\delta \theta_h$) in the case of the encasing steel tube (Fig. 7). Assuming a value for neutral-axis, forces and moments are summed over the entire area of the cross-section in an attempt to achieve equilibrium. Through an iterative process, the location of the neutral axis is determined as the one ensuring sectional equilibrium of forces, following which the moments are determined. A simple computer program has been developed to perform the numerical analysis, and can further be extended to determine points on the column interaction curves for any combination of design parameters.

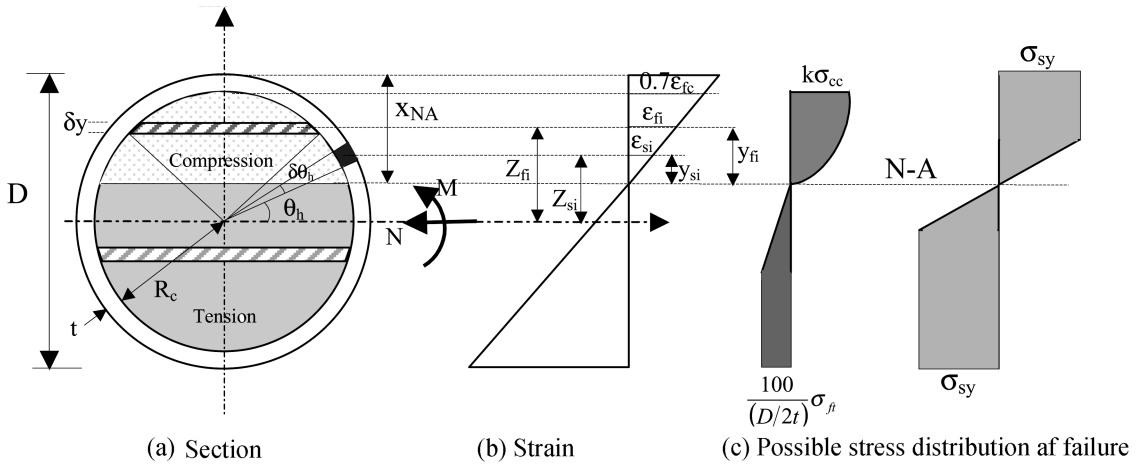


Fig. 7 Proposed strain and stress distributions

Basic assumptions made include;

- Plane sections before bending remain plane after bending, implying that the strain in the fill material and the steel tube are linearly proportional to the perpendicular distance from the neutral axis
- Failure occurs when the extreme compressive strain in the fill material reaches a limiting value $0.7 \epsilon_{cc}$ where ϵ_{cc} is the strain at confined strength of fill material
- Shear and torsion stresses are neglected
- Good bond exists between steel and concrete
- Fill material and steel characteristics are assumed as given in Fig. 8. There is some residual tensile strength of the fill material (σ_{ft}), which is further enhanced by the confining effect of the encasing steel tube to give a total tensile effect or tension stiffening equal to $\{100/(D/2t)\} \sigma_{ft}$. An elasto-plastic response is assumed for the steel component, where the compression regime is taken as elasto-perfectly plastic and the tension regime is taken as bilinear. It is to be noted that even though fiber analysis requires only uniaxial constitutive relationships, the response of steel in composite structures is the result of complex multiaxial effects.

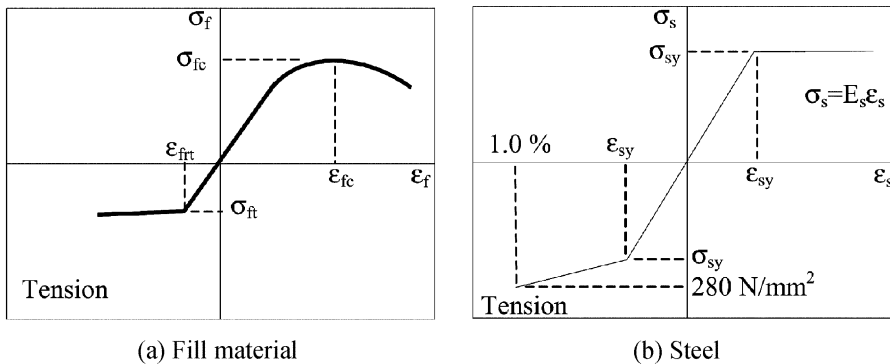


Fig. 8 Material stress-strain relations

For equilibrium,

$$N_u = \int_{A_f} \sigma_f(\varepsilon_f) dA_f + \int_{A_s} \sigma_s(\varepsilon_s) dA_s = 0 \quad (\text{hence locate } N - A)$$

$$M_u = \int_{A_f} \sigma_f(\varepsilon_f) Z_{fi} dA_f + \int_{A_s} \sigma_s(\varepsilon_s) Z_{si} dA_s \quad (10)$$

where Z_{fi} and Z_{si} are elemental lever arms of forces measured from the center of section. The elemental areas are; $\delta A_f = 2(R_c^2 - Z_{fi}^2)^{0.5} \delta y$ and $\delta A_s = (D/2 - t/2)(\delta \theta_h) t$

Due to compatibility of deformations, the strains at different levels can be related to curvature (ϕ) by;

$$\frac{\varepsilon_{fi}}{y_{fi}} = \frac{\varepsilon_{si}}{y_{si}} = \frac{0.7\varepsilon_{fc}}{x_{NA} - t} = \phi \quad (11)$$

The stress-strain relation for the confined fill material in compression is assumed to be defined by following equation as given in Fig. 8.

$$\sigma_f = \frac{\sigma_{fc} \left(\frac{\varepsilon}{\varepsilon_{fc}} \right)^r}{r - 1 + \left(\frac{\varepsilon}{\varepsilon_{fc}} \right)^r} \quad (12)$$

where

$$r = \frac{E_c}{E_c - \frac{\varepsilon}{\varepsilon_{fc}}} \quad \sigma_{fc} = \sigma_{fk} + 4.1 \sigma_l \quad \sigma_l = \frac{\varepsilon_{fb} \nu_f K}{\varepsilon_{fu} G} \frac{2t \sigma_{sy}}{(D - 2t)}$$

$$\varepsilon_{fc} = \begin{cases} \varepsilon_{fu} \left[1 + \frac{20 \sigma_l}{\sigma_{fk}} \right] & \text{for LCM2 and CN} \\ \varepsilon_{fu} \left[1 + \frac{40 \sigma_l}{\sigma_{fk}} \right] & \text{for E1A} \end{cases}$$

E_c = Modulus of elasticity of fill material; ν_f = Poisson's ratio of fill material

σ_{fc} = Confined strength of fill material; σ_{fk} = Unconfined strength of fill material

σ_l = lateral confining pressure of fill material at ultimate confined strength

σ_{fi} = residual tensile strength of fill material; ε_{fc} = Strain at confined strength of fill material

ε_{fu} = Strain at unconfined strength of fill material; ε_{fi} = Strain at residual tensile strength of fill material; ε_{fb} = Undefined strain quantity, probably fill material axial strain at yielding of biaxial steel; $K = E/3(1 - 2\nu_f)$ Bulk modulus; $G = E/2(1 + \nu_f)$ Shear modulus

Table 5 Nominal values assumed for analysis

Fill material description	Fill material designation	ε_{fb} (%)	σ_{fi} (N/mm ²)	ε_{fi} (%)
Latex cement mortar	LCM2	1.3	3.0	0.025
Epoxy concrete-HS	E1A	0.35	4.5	0.2
Normal concrete	CN	1.4	3.5	0.025

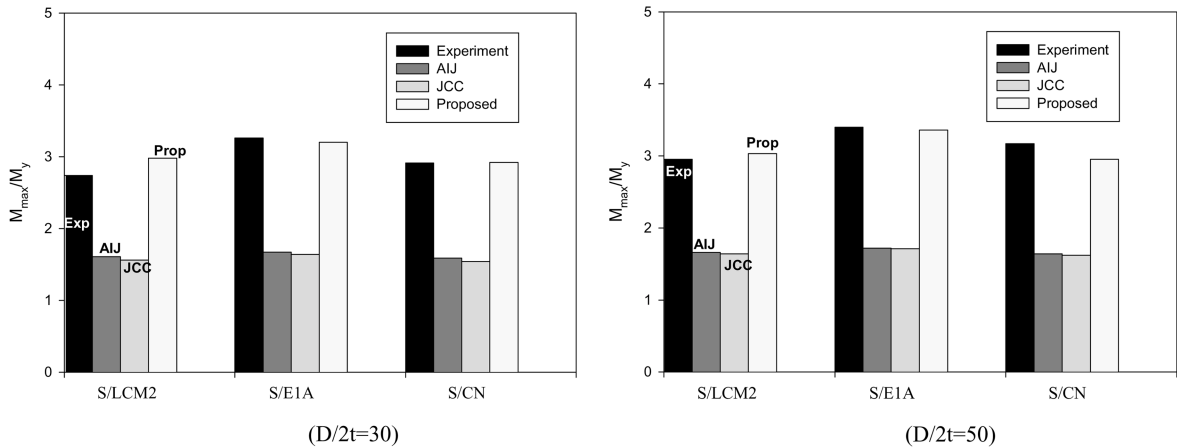


Fig. 9 Analyzed and experimental normalized ultimate moments

Fig. 9 clearly shows that the proposed method predicts the ultimate flexural strength of the composite beams much better than the AIJ or JCC methods. This is because the proposed method realistically takes into account the confined strength as well as the tension stiffening effect of the fill material. It is apparent that the benefit of increased confinement due to end-plates is quite substantial and needs to be optimized in design. At the moment, large discrepancies between various design codes exist in terms of geometric and strength parameters, even when the same design philosophy is adopted, indicating the need for more accurate design guidelines. Further, with development of high strength concrete and structural steel, there is need to develop a good understanding of the fundamental behaviour. Using the proposed fiber section analysis method, it is possible to generate moment-axial load ($M-N$) interaction curves for given parameters.

4. Conclusions

In close conformity with results from previous compressive tests on stub columns, bending tests have further reaffirmed the immense potential of the more durable polymer-based fill materials as complementary fill materials to cement concrete for enhanced stiffness, strength and ductility. It is presented that:

- Epoxy polymer concretes produce composite steel beams of much increased strength and/or ductility.
- Epoxy polymer concretes, due to their varied material properties, produce composite beams of diverse characteristics hence presenting the construction industry with a broadened horizon of application. For example epoxy concrete E1A would supplement ordinary concrete for high strength composite structures, while epoxy concrete E2A would complement ordinary concrete for structures whose design is ductility-based.
- A proposed method based on strain compatibility and equilibrium of sectional forces and moments can predict the ultimate bending moment adequately and much better than current procedures given in national or continental codes.

Future work should seek to provide means of reducing the high cost of polymers, through inclusion of municipal wastes in eco-friendly polymer blends. In addition, appropriate life-cycle costing techniques

ought to be developed to take advantage of the range of properties offered by polymers, especially with regard to durability and resistance against aggressive environments.

Acknowledgements

The authors are most grateful to the Ministry of Education, Science, Sports and Culture, Japan, and the Japan Society for the Promotion of Science (JSPS).

References

- Abdel-Fattah, H. and El-Hawary, M. (1999), "Flexural behaviour of polymer concrete", *J. Construction and Building Materials*, **13**, 253-262.
- Architectural Institute of Japan (AIJ) (1997), Recommendations for design and construction of concrete filled steel tubular structures.
- Bentur, A. (2002), "Cementitious materials - Nine millennia and a new century: Past, present, and future", *J. Mat. Civil Engrg.*, ASCE, **14**(1), 2-22.
- Fowler, D.W. (1999), "Polymers in concrete: A vision for the 21st century", *Cement and Concrete Composites*, **21**, 449-452.
- Hastak, M. and Halpin, D.W. (2000), "Assessment of life-cycle benefit-cost of composites in construction", *J. Composites for Construction*, ASCE, **4**(3), 103-111.
- Joint Committee of steel-concrete composite structures, JSCE (1999), "Theory and design of steel concrete hybrid structures: Part 1: Theory and basic concept", edited by Sonoda, K., 109-136.
- Kardon, J. (1997), "Polymer-modified concrete: Review", *J. Mat. Civil Engrg.*, ASCE, **9**(2), 85-92.
- Kawashima, K. and Unjoh, S. (1997), "Impact of Hanshin/Awaji earthquake on seismic design and seismic strengthening of highway bridges", *J. Struct. Mech.*, JSCE, 1-30.
- Kitada, T. (1998), "Ultimate strength and ductility of state-of-the-art concrete-filled steel bridge piers in Japan", *Eng. Struct.*, **20**(4-6), 347-354.
- Nakanishi, K., Kitada, T. and Nakai, H. (1999), "Experimental study on ultimate strength and ductility of concrete filled steel columns under strong earthquake", *J. Const. Steel Res.*, **51**, 297-319.
- Ohama, Y. (1987), "Principle of latex modification and some typical properties of latex-modified mortars and concretes", *ACI Mat. J.*, **84**(6), 511-518.
- Ohtani, Y. and Matsui, S. (1997), "Stability problems in steel-concrete composite members and elements, structural stability design: Steel and composite structures", edited by Fukumoto, Y., Elsevier Science, London 229-251.
- Oyawa, W.O., Sugiura, K. and Watanabe, E. (1998), "Elasto-plastic behaviour of axially loaded filled circular steel stub columns", *J. Struct. Engrg.*, JSCE, **44A**, 147-158.
- Oyawa, W.O., Sugiura, K. and Watanabe, E. (1999), "Flexural deformation characteristics of filled steel beams subjected to pure bending", *J. Struct. Engrg.*, JSCE, **45A**, 105-116.
- Oyawa, W.O., Sugiura, K. and Watanabe, E. (2001), "Polymer concrete in filled steel composite members under compressive load", *J. Construction and Building Materials*, Elsevier Science, 187-197.
- Rebeiz, K.S. and Mielich, K.L. (1995), "Construction use of municipal-solid-waste ash", *J. Energy Engrg.*, ASCE, **121**(1), 2-13.
- Rebeiz, K.S. and Fowler, D.W. (1996), "Flexural strength of reinforced polymer concrete made with recycled plastic waste", *ACI Struct. J.* **93**(5), 524-530.
- Reddy, B.D. (1979), "An experimental study of the plastic buckling of circular cylinders in pure bending", *Int. J. Solids Struct.*, **15**, 669-683.
- Shams, M. and Ala, S.M. (1997), "State-of-the-art of concrete-filled steel tubular columns", *ACI Struct. J.*, **94**(5), 558-571.

- Solovjov, G.K., Trambovestky, V.P. and Kruger, D. (1994), "Furan resin polymer concrete in the commonwealth of independent states (CIS)", *ACI Mat. J.*, **91**(2), 158-160.
- Spacone, E. and El-Tawil, S. (2004), "Nonlinear analysis of steel-concrete composite structures: state of the art", *JSE, ASCE*, **130**(2), 159-168.
- Sujjavanich, S. and Lundy, J.R. (1998), "Development of strength and fracture properties of styrene-butadiene copolymer latex-modified concrete", *ACI Mat. J.*, **95**(2), 131-143.

CC